Magnetoresistive Biosensors for On-Chip Detection and Localization of Paramagnetic Particles

Zhaochen Yin, *Student Member, IEEE*, Edoardo Bonizzoni, *Member, IEEE*, and Hadi Heidari, *Senior Member, IEEE*

***Abstract*—This paper presents the design and the implementation of an on-chip magnetoresistive sensors array for cell detection and localization. Giant magnetoresistance (GMR) sensors have been used due to their high sensitivity and resolution. A new calibration and localization algorithm has been coded and implemented. In order to generate the required homogenous magnetic field, a custom 3-D printed Halbach cylinder has been simulated and characterized. The system includes sensory and electronic boards to collect the data and to transfer them to a computing server. The experimental results are displayed in a visual interface. Ferrofluid is used to model and simulate the magnetic field change of the cell. This paper demonstrates a 4 × 4 sensor array and provides a step toward the miniaturized on-chip magnetoresistive-based cell detection and localization for portable diagnostics applications.**

***Index Terms*—Magnetic biosensors, giant magnetoresistive (gmr), lab-on-chip, detection, localization, paramagnetic particles, point of care (PoC), diagnostics.**

I. Introduction

RECENTLY, the use of biosensors has experienced rapid growth for applications like point-of-care (PoC) testing, disease diagnosis, and immunoassays [1]. The PoC diagnostic provides a convenient way to diagnose diseases everywhere towards personalised healthcare technologies, for home and clinical deployment [2]. These portable devices are used for fast and early detection of diseases and for treatments efficiency optimisation. As an example, among many other applications, biosensors are more widely used in PoC systems for cancer cells early detection [3]. There are various pioneer technologies in the development of biosensor-based diagnoses, like magnetic, ultrasonic, photonics, and others. A magnetic-based immunoassay is a type of diagnostic tool that uses magnetic beads as labels, involving specific bindings of an antibody and its antigen. In this process, magnetic sensors are used for antibody–antigen binding selection and localization [4]–[6]. Recent advances have allowed the integration and multiplexing of magnetic sensors onto sub-mm CMOS chips toward magnetic-based diagnostics miniaturization [7]–[9].

This paper focuses on magnetic-based biosensors for localisation and detection of paramagnetic particles using giant magnetoresistance (GMR) sensors as an optimal choice for PoC applications due to their high sensitivity and low offset. Table I summarizes and compares the main features of recent miniaturized GMR-based biosensing systems, including this work [10]–[14]. Fig. 1 conceptually illustrates the basic multilayered structure of GMR sensors: It consists of two magnetic material layers sandwiching a non-magnetic interlayer. The magnetic layers are designed to have an anti-ferromagnetic coupling (i.e., the magnetisation of these layers is opposite to each other when there is no external magnetic field applied to the material). Extending the preliminary work reported in [15], this paper presents the results from an extensive physical simulation, extends the number of sensors in the array from 3 × 3 to 4 × 4, and provides guidelines for sensors calibration and performance optimisation. The employed 4 × 4 sensors array are off-the-shelf GMR chips. The achieved simulation and experimental results demonstrate the effectiveness of the approach for future miniaturised magnetic-based diagnostics. This approach is particularly remarkable in comparison with the existing bulky and costly diagnostic systems.

This paper is organised as follows. A brief state-of-art overview of recently reported magnetic-based biosensors including biomagnetic sensing and cell detection is presented in Section II. Section III describes the design and the main features of the selected sensors, of the electronic interface, and the used Halbach cylinder. Section IV provides detailed simulation results of the cell detection achieved with GMR sensors, along with the uniform magnetic field generated by the designed Halbach cylinder. Section V discusses the collected experimental results, while the key outcomes are finally summarized in Section VI.

II. Giant Magnetoresistance Biosensors

GMR sensors can be conveniently used for biological and chemical targets detection. However, before detection, magnetic

Manuscript received April 10, 2018; revised June 9, 2018 and July 6, 2018; accepted July 7, 2018. Date of publication July 23, 2018; date of current version August 22, 2018. This work was supported by the Royal Society under Grant "MAGLAB" RSG\R1\180269. This paper was presented in part at the 2017 IEEE Sensors Conference, Glasgow, U.K., October 30–November 1. *(Corresponding author: Edoardo Bonizzoni.)*

Z. Yin was with the Microelectronics Lab, School of Engineering, University of Glasgow, Glasgow G12 8QQ, U.K. He is now with the Department of Electrical, Computer and Biomedical Engineering, University of Pavia, Pavia 27100, Italy (e-mail: zhaochen.yin01@universitadipavia.it).

E. Bonizzoni is with the Department of Electrical, Computer and Biomedical Engineering, University of Pavia, Pavia, Pavia 27100, Italy (e-mail: edoardo.bonizzoni@unipv.it).

H. Heidari is with the Microelectronics Lab, School of Engineering, University of Glasgow, Glasgow G12 8QQ, U.K. (e-mail: Hadi.Heidari@glasgow.ac.uk).

Color versions of one or more of the figures in this paper are available online at http://ieeexplore.ieee.org.

Digital Object Identifier 10.1109/JERM.2018.2858562

TABLE I
COMPARISON OF THE STATE-OF-THE-ART GMR-BASED BIOSENSING SYSTEMS

Type	Detection	Sensor Array	Sensitivity	Application	Reference
GMR Biosensor Array	Magnetorelaxation	8 × 10 GMR sensor array	1 Ω/Oe.	Point-of-Care (PoC) diagnostics platform.	[8]
Integrated GMR biosensor	Biomarkers	N/A	Sensitive detection of AFP from 1 to 10 ng/ml	GMI-based MIA in clinical trials	[9]
Frequency-shift magnetic biosensors	Single-bead sensitivity	8 parallel sensor cells	80 beads	Point-of-Care (PoC) molecular-level diagnosis	[10]
3D field sensor with single bridge of spin-valve GMR films	Biomarkers	N/A	B_X 30V/T B_y 18V/T B_z 8.5V/T	Electronics, electrical, and navigation	[11]
CPP-GMR Spin-Valve Sensors	Magnetic bits	N/A	R/R up to 14% w	Ultra-high-density magnetic recording	[12]
GMR Sensors Array	Ferrofluid	4 × 4 sensor array	2 T^{-1}	Cell detection and localisation	This work

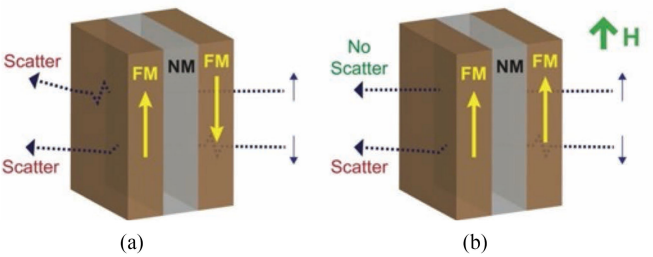

Fig. 1. Working principle of GMR multilayers structures.

particles immobilisation on the sensor has to be performed. This is commonly achieved by exploiting biomolecular interactions (e.g., antigen-antibody), and thus requires functionalisation via biological or chemical treatments. This section provides a brief overview of the state-of-the-art for both bio-magnetic sensing and cell detections.

A. Biomagnetic Sensing

A biosensor is a device for analysis that uses an electronic output signal, generated by a biological molecular recognition component, to drive a transducer [16]. Magnetoresistive biosensors provide a promising method for biomedical detections: they use magnetic particles to localise and sort diagnoses. Such sensors offer a low-cost, fast and robust sensing system with higher sensitivity when compared with enzyme-linked immunosorbent assays and fluorescence-based methods which are nowadays widely used in clinical environments [17]. Magnetoresistive biosensors are at the state-of-the-art studied in three directions: *(i)* develop the synthesis of magnetic beads that can have the same characteristics of microarrays; *(ii)* employ biosensors in high-resolution, on-chip electrostatic or magnetic field gradient architectures, which can manipulate functionalised single magnetic beads; and *(iii)* employ biocompatible solid-state biosensors for quantifying magnetic beads [18].

In the last few years, magnetoresistance biosensing platforms such as GMR and tunnelling magnetoresistance (TMR) sensors experienced rapid growth and can be employed in a wide variety of medical applications: point-of-care clinical diagnostics, developments in pharmaceutical drugs, DNA analytics, etc. [19]. However, accurate analysis of biological samples needs further process and trained technicians, increasing both the cost and the time of the measurement. This paper provides a significant improvement in overcoming the above limits proposing a portable and rapid GMR biosensor platform with calibration and localization algorithm.

B. On-Chip Cell Detection

Due to the universalisation and request of robust and portable biosensors, there is a tremendous demand for lab-on-chip products that do not need expensive specialised equipment or personnel to perform the analysis. This brings in the need for methods to separate, to manipulate, and to move specific particles to specific positions. Microfluidics has been a conventional method for particles manipulation, but there have been studies on using magnetic sensor-manipulator systems as selective and fast analytical devices [20], [21]. On-chip GMR sensors represent a powerful and low-power sensing system choice featuring high sensitivity and making cell detection easy-to-use and faster. Other healthcare technologies based on on-chip GMR sensors for early detection of diseases have been developed over the past few years [22]. Furthermore, due to the fast development of very large-scale integration technologies and multiplex technologies, the fabrication cost of GMR-based sensors significantly reduced. GMR sensors can be conveniently arranged in a large array to determine the location of cells by detecting the difference of the magnetic field density from adjacent sensors [23], [24]. GMR sensors, by measuring the magnetic field generated by magnetic particles binding to the cells, open potential applications in biological cell sorting and localisation. For example, it has been demonstrated that GMR-based

biosensors can detect the influenza A virus [22] and can quantify the kinetics of antibody–antigen binding [25].

III. Design and Implementation

The developed prototype includes GMR sensors with readout interface and Halbach cylinders to generate the required uniform magnetic field. The Halbach cylinders have been custom designed, 3-D printed, and arranged suitably around the sensors array. Ideally, all the sensors should provide the same output value in the presence of the generated uniform magnetic field. The ferrofluid has been used in a pipette to emulate magnetic nanoparticles. GMR sensors measure the magnetic field via a change in the sensor resistance, thereby enabling cells detection and localization.

A. Sensors Selection

This experiment aims to realise the function of cell localisation and sorting. Two types of analogue and digital GMR sensors have been considered. The analog sensor can read the magnetic flux density to display changes of the magnetic field as an analogue output signal. On the other hand, the digital GMR sensor can detect the magnetic field and show its actual value in a digital format. This experiment needs to read the magnetic field variations and then determine its applicable strength. Therefore, the analogue GMR sensor is the optimal choice to demonstrate the magnetic field variations as an output signal based on the flux density. This project uses off-the-shelf NVE's analogue GMR sensors with 12%–16% resistance change, as a model choice for proof-of-concept [26].

B. Hysteresis

The ferromagnetic materials in GMR multilayer are prone to the hysteresis, i.e., a given magnetisation is not reset when the imposed magnetising field is removed.

Hysteresis represents an issue in applications in which the applied magnetic field varies randomly, like in the case here considered for cell detection and localisation. Particularly, in this case of the design, hysteresis causes an offset in the output voltage of the sensors readout circuits. Indeed, with 5-V power supply, a single cube magnet was used to test the hysteresis. The measured saturated value and the hysteresis value have been 0.27 V and 0.01 V, respectively. However, thanks to the large linear range and high sensitivity of the GMR sensors, the 4% hysteresis error at the output voltage is acceptable and provides enough accuracy for localisation.

C. Uniform Magnetic Field

This experiment, as mentioned, utilises a ferrofluid, magnetised in a uniform magnetic field. There are two methods to generate a uniform magnetic field: using a Helmholtz coil or using Halbach cylinders. Since the Helmholtz coil is too bulky to be used in a portable device, to minimize the system size, a custom 3-D printed Halbach cylinder, consisting of 16 cube magnets [27] has been employed in our design approach.

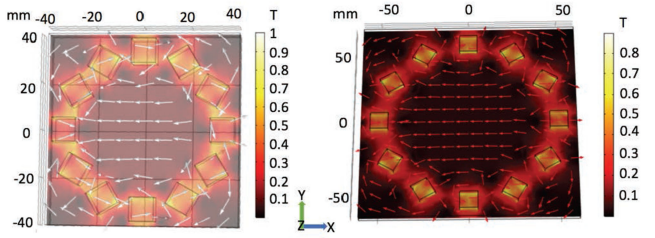

Fig. 2. (Left) COMSOL simulation result for the Halbach cylinder (radius 3.3 cm). (Right) COMSOL simulation result for the Halbach cylinder (radius 5 cm).

The design of the Halbach cylinder has been optimised through extensive finite-element method (FEM) based simulations, which considered different diameters ranging from 3.3 cm to 5 cm. The custom cylinder has been designed in SolidWorks. The 3-D printed Halbach cylinder is portable and generates a uniform magnetic field up to 700 mT.

IV. Simulation Results

FEM allows taking into account nonlinear magnetic properties, detailed geometries and distributed currents excitation. Therefore, it offers high accuracy in electromagnetic design in comparison to other methods. In this design, the software COMSOL Multiphysics has been used to run the finite element analysis to fine-tune, verify, and evaluate the performance of the Halbach cylinder and the ferromagnetic beads positioning on top of the GMR sensors.

In the Halbach cylinder simulations, 16 cube magnets were considered and modelled to generate the required uniform magnetic field. For each magnet, the angle difference is considered as 22.5 degrees with 45 degrees rotation. Simulations ensure that the cylinder can adequately generate a uniform and stable magnetic field for operating the GMR sensors at their sensitivity axis. In the simulations, the considered environment is air and all the boundaries are set at a zero-potential point. The magnets embedded in the Halbach cylinder were N42 neodymium magnets that are strong and versatile cube magnets with the size of $10 \times 10 \times 10$ mm. Fig. 2 shows the simulation results collected from COMSOL for Halbach cylinders with different radius. The magnets position on the cylinder was localised correctly based on calculations, and confirmed by COMSOL simulations. It can be noted that it is possible to generate a uniform magnetic field over 95% of the internal diameter of the cylinder. To avoid the interference of non-uniform magnetic field in the edges of the cylinder, a stable 3-D printed cage has been used where the Halbach cylinder is placed at the top.

Furthermore, COMSOL has been used to investigate the considered GMR sensor behaviour over a specific position of ferrofluid particles. The simulation results are used to find out an optimised solution for detection of ferromagnetic beads. The simulation results in Fig. 3 show the operated movements of ferromagnetic beads on top of GMR sensors following two trajectories (X and Y axis). The model box built in this simulation is a cylinder instead of a cube to avoid any error due to the different boundary shape. The radius of this cylinder is 20 μm

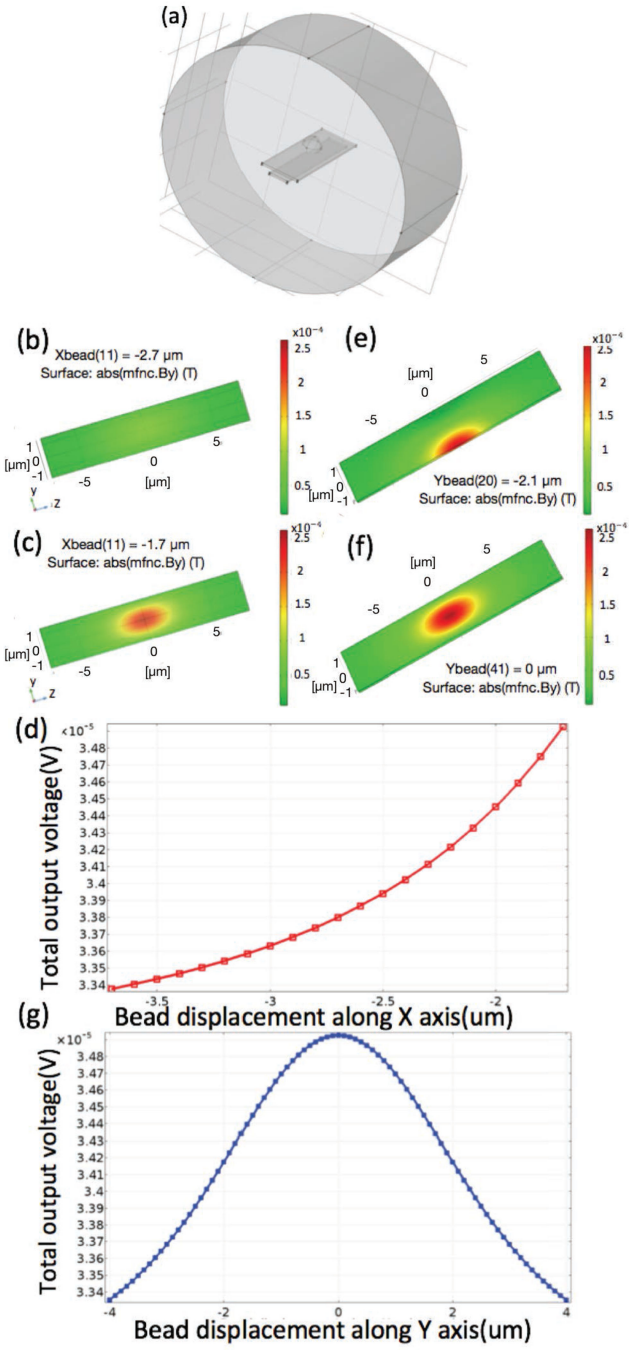

Fig. 3. (a) Model box structure of the magnetic biosensor in COMSOL. (b)–(c) Total output voltage while the ferromagnetic bead moves at X axis and (d) output voltage of the bead along X axis. (e)–(f) Total output voltage while the ferromagnetic bead moves at Y axis and (g) output voltage of the bead along Y axis.

and its height is 15 μm. The work plane of this cylinder is the XY plane. The material of the model box is defined to be air. The GMR sensor is modelled inside the model box with 3-μm width, 15-μm depth, and 0.3-μm height. For real sensor devices, the structure of the GMR element has several layers with different materials, but in simulation, the material was set to be Permalloy which is a nickel (about 80%) and iron (about 20%) magnetic alloy.

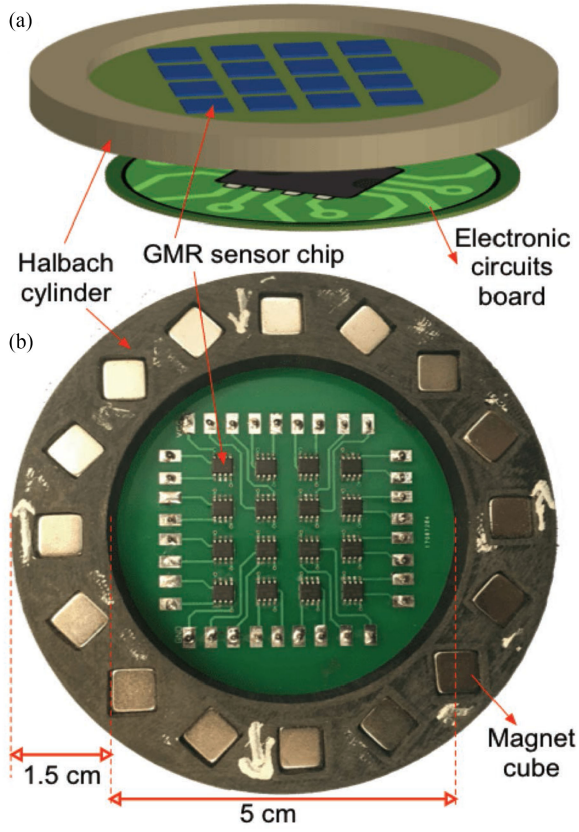

Fig. 4. (a) Final prototype multi-level including the sensory and electronic circuits boards. (b) Top view of the developed 4 × 4 sensors array surrounded by the 3-D printed Halbach cylinder.

The X trajectory moves the magnetic bead from one extreme to a position close to the conducting line. The result shows that when the magnetic bead moves, the stray field produced by the magnetic bead is increased. As a result, the output voltage is increased as well. The Y trajectory moves the magnetic bead from one edge of the conducting line to another edge with the same distance between the bead and the conducting line. During this movement, the simulated output voltage is reported in Fig. 3(f) and ranges between 33.4 μV and 34.9 μV. As a result, the measured magnetic flux density on the GMR sensor is affected by the conducting lines. The simulated Y components of the magnetic flux density on the surface of the conducting line and of the GMR are 2.8948 mT and 2.5587 mT in average, respectively.

V. Experimental Results

The fabricated prototype includes two boards; one hosts the array of GMR sensors covered by a protective coating layer and the other is dedicated to the electronic readout circuit interface. Fig. 4 shows the boards arrangement and a picture of the prototype. The sensory board includes pins for proper connections between the readout circuit and the sensors. The two boards are surrounded by 3-D printed Halbach cylinder.

A. Sensor Calibration and Localisation Algorithm

The sensors, in an array configuration mounted onto the surface of the board, will never be in a perfectly uniform arrangement. Additionally, they will never altogether sense a perfectly uniform field. Calibration is performed to overcome such issues and to avoid mismatch among sensors so that all the sensors will have a similar range to work with.

In this project, the sensors will be calibrated by initially finding the maximum value of the sensor, and then subtracting the baseline value. This will give to each sensor a viable operating range. The localization algorithm will then be created under the assumption that the operating range will function similarly for all of the calibrated sensors. For example, a magnet is placed in a specific distance from sensor '*1*,' and sensor *'1'* gives an output of 50% its operating range. Now if sensor *'2'* is brought in from a large distance until it also gives an output of 50% its operating range, then the distance between sensor *'1'* and the magnet, and sensor *'2'* and the magnet should be the same.

Various algorithms for localisation in both 2-D and 3-D space have been developed to minimise errors, optimise location and detection, and provide comprehensive guides on producing tracking mechanisms [28], [29]. For this project, a simpler algorithm was designed in order to ensure a working model was developed on time. The algorithm is implemented with two functions for cell detection and localisation. The 4 × 4 GMR sensor array configuration is utilised in this project, and then the detection can be realised by comparing the magnetic field changes with the biological data to distinguish the cells. It can also be applied to collect the magnetic field data in specified cells for cell sorting and patterning.

The algorithm used in this project is referred to as weighted average algorithm. It works by using the output of the sensors to "pull" a circle towards its specific coordinates. The stronger the output, the higher weighting will be given to that particular sensor, resulting in a stronger pull. Mathematically, the situation can be modelled as follows:

$$\mathrm{x_{wa}} = \sum_{1}^{n} \frac{\mathrm{v_i}}{\mathrm{maxv_i} - \mathrm{minv_i}} \cdot \mathrm{x_i} \tag{1}$$

$$\mathrm{y_{wa}} = \sum_{1}^{n} \frac{\mathrm{v_i}}{\mathrm{maxv_i} - \mathrm{minv_i}} \cdot \mathrm{y_i} \tag{2}$$

where $\mathrm{x_{wa}}$ and $\mathrm{y_{wa}}$ are the weighted positions of the detection point at X axis and Y axis respectively. i refers the number of the sensor and V_i is the output voltage of the ith sensor. This algorithm is suitable for large sensor array because it will diminish the shift in detection.

The developed software comprises a user interface that helps calibrating the system and easily visualizing the cell localisation. The GMR sensors need to be calibrated before entering the localisation procedure. The calibration interface panel allows the user in choosing the number of sensors (see Fig. 5(a) and (b)) and allows registering for each sensor its maximum and minimum output voltage value. The maximum value is measured when the ferrofluid is placed on top of the sensor, while the minimum value is recorded in the absence of the ferrofluid.

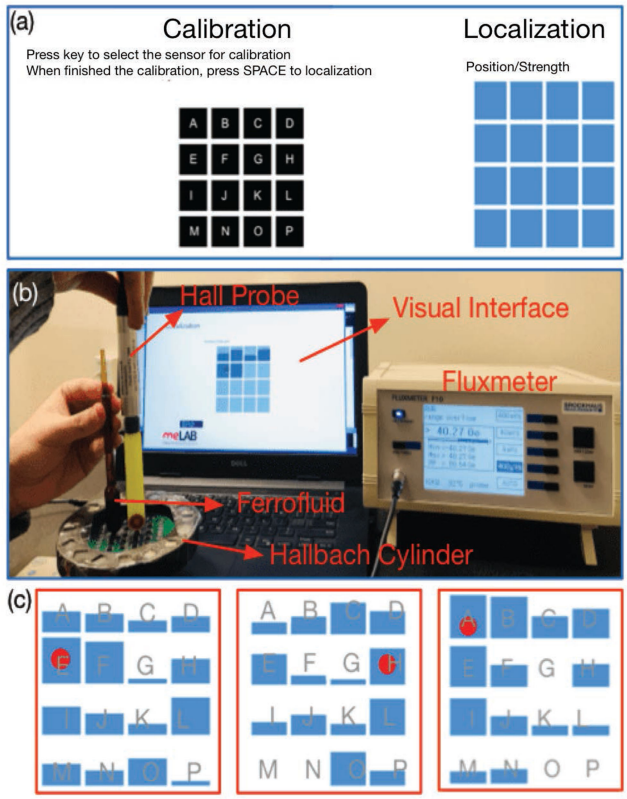

Fig. 5. (a) Visual interface design for calibration and localisation. (b) Test setup and (c) ferrofluid detection and localization for 4 × 4 sensors detect system at different positions.

These values will be accounted for during the localisation procedure. The localisation user interface is reported in Fig. 5(c). The matrix represents the 16 sensors (labelled from A to P) and their placement. A bar, associated to each sensor, displays the strength of the GMR sensor while the red point specifies the position of ferrofluid.

The software has been implemented and coded in a microcontroller for data collection. The Processing Development Environment (PDE) was used to sketch the 2-D visual interface [30]. The implemented codes include six segments: display data, pages, serial, calibration, classification and localization.

B. Test and Measurement

For comparison with the FEM simulation results in Section IV, various measurements were taken of both the magnets themselves and various locations inside the Halbach cylinders. For the tests of only magnets, the field was measured by touching the Brockhaus Hall probe (Field Coil) to the top of the magnet. The Hall probe was moved around to find the spot of highest magnetic flux density. It is essential to account for the imperfections that are present in all permanent magnets, and so an average value was obtained from after measuring four different magnets to be 0.32 T. In average, the actual field strength values are >90% of the FEM field strength. This indicates a good agreement between the measurements and simulations. The existing difference is probably because of the magnetic

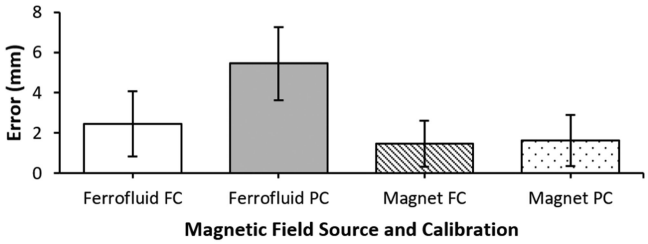

Fig. 6. Comparison of error in localization from actual position for different magnetic sources and calibrations. Ferrofluid tests show mean (SD) of 2.45 (1.61) mm and 5.45 (1.82) mm for FC and PC. Magnet tests give 1.48 (1.14) mm and 1.62 (1.26) mm.

material parameters for N42 neodymium which is used during FEM analysis and found to be not the same as the parameters of the actual magnet.

Fig. 6 shows the measured stable and accurate outputs collected from the 4×4 sensor array with both magnet and ferrofluid. The system can be fully or partially calibrated. In the full calibration mode, both minimum and maximum values are calibrated, while the partial calibration mode assumes zero as minimum value. By comparing the actual location of the ferrofluid source with the acquired digital output, mean standard deviation (SD) errors of 2.45 (1.61) mm and 5.45 (1.82) mm were observed in full calibration (FC) and partial calibration (PC), respectively. This corresponds to mean error areas of 3.0% and 14.9%, respectively, calculated on the 25×25 mm^2 array surface. In the case of used magnet source, the measured mean errors have been 1.48 (1.14) mm and 1.62 (1.26) mm in FC and PC, respectively. These correspond to mean error areas of 1.1% and 1.3%. Although the error in PC ferrofluid test is high, the rest of detection results shows consistent and precise localization. This illustrates the importance of proper calibration and also demonstrates the effectiveness of the proposed approach for both a robust ferromagnetic source and a paramagnetic material:

The sensitivity (S) of the sensor can be estimated with the following expression:

$$S = \frac{V_{in}}{B} \tag{3}$$

where V_{in} is to the measured output voltage, and B is the detected magnetic field.

Fig. 7(a) and 7(b) illustrate the measured sensitivity in the presence of a uniform magnetic field. It ranges from 0.2 to 2.3 V/T and from 0.9 to 3 V/T in absence or presence of the ferrofluid, respectively. In this experiment, the sensors have already been calibrated. However, due to the PCB design and fabrication, the sensitivity might be changed. To make sure that the output for each GMR sensor can be reliable on detection without large shift, the sensitivity test has been performed under uniform magnetic field with and without ferrofluid. The sensitivity variation for each sensor is not significant (less than 0.2 V/T). This small change will not affect the position shift on detection result significantly. These results also confirm that the measured voltages at the output of the GMR sensors are higher in presence of the ferrofluid, as outlined in Fig. 7(c). Besides,

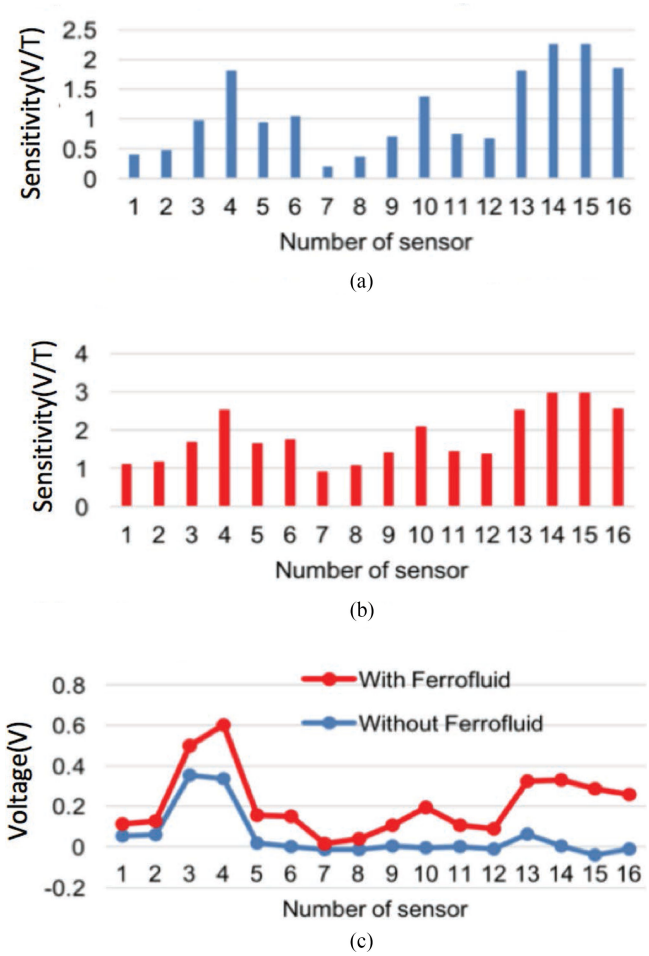

Fig. 7. Measured sensitivity of GMR in uniform magnetic field (a) without and (b) with ferrofluid. (c) Comparison of the voltage measured in presence of uniform magnetic field with or without ferrofluid.

notice that all the measured sensors exhibit the same behaviour. The only exception is sensor number 15 that shows a negative voltage because of voltage fluctuation.

VI. Conclusion and Outlook

This paper presented the design of a prototype developed for on-chip cell detection and localisation based on magnetic sensors. The sensory board includes a 4×4 GMR sensors array. The ferrofluid and a customised 3-D printed Halbach cylinder was employed to simulate the magnetic field change in the bead. Sensory chips could detect an average magnetic sensitivity of 2 V/T at room temperature. The implemented algorithm helps in achieving higher sensitivity, positioning speed, and accurate calibration of the GMR sensors.

As future work, the GMR sensors will be integrated into a single chip using standard CMOS technology, and the results will be compared with the measured data in this paper. The miniaturisation will provide a 3-D environment rather than a 2-D one in sensor testing for the applications of cell sorting and actual distance determination.

REFERENCES

[1] A. Niemz, T. M. Ferguson, and D. S. Boyle, "Point-of-care nucleic acid testing for infectious diseases," *Trends Biotechnol.*, vol. 29, pp. 240–250, 2011.

[2] J. Wannenburg and R. Malekian, "Physical activity recognition from smartphone accelerometer data for user context awareness sensing," *IEEE Trans. Syst., Man, Cybern. Syst.*, vol. 47, no. 12, pp. 3142–3149, Dec. 2017.

[3] F. T. Fischbach and M. B. Dunning, *A Manual of Laboratory and Diagnostic Tests*. Baltimore, MD, USA: Lippincott, 2009.

[4] V. Nabaei, R. Chandrawati, and H. Heidari, "Magnetic biosensors: Modelling and simulation," *Biosens. Bioelectron.*, vol. 103, pp. 69–86, 2018.

[5] M. D. Tarn and N. Pamme, "On-chip magnetic particle-based immunoassays using multilaminar flow for clinical diagnostics," *Microchip Diagnostics, Methods Protocols*, vol. 1547, pp. 69–83, 2017.

[6] D. A. Hall *et al.*, "GMR biosensor arrays: A system perspective," *Biosens. Bioelectron.*, vol. 25, pp. 2051–2057, 2010.

[7] H. Heidari, E. Bonizzoni, U. Gatti, and F. Maloberti, "A CMOS current-mode magnetic hall sensor with integrated front-end," *IEEE Trans. Circuits Syst. I, Reg. Papers*, vol. 62, no. 5, pp. 1270–1278, May 2015.

[8] H. Heidari, E. Bonizzoni, U. Gatti, F. Maloberti, and R. Dahiya, "CMOS vertical Hall magnetic sensors on flexible substrate," *IEEE Sensors J.*, vol. 16, no. 24, pp. 8736–8743, Dec. 2016.

[9] K.-M. Lei, H. Heidari, P.-I. Mak, M.-K. Law, F. Maloberti, and R. P. Martins, "A handheld high-sensitivity micro-NMR CMOS platform with B-field stabilization for multi-type biological/chemical assays," *IEEE J. Solid-State Circuits*, vol. 52, no. 1, pp. 284–297, Jan. 2017.

[10] X. Zhou, C.-C. Huang, and D. A. Hall, "Giant magnetoresistive biosensor array for detecting magnetorelaxation," *IEEE Trans. Biomed. Circuits Syst.*, vol. 11, no. 4, pp. 755–764, Aug. 2017.

[11] T. Wang, Z. Yang, C. Lei, J. Lei, and Y. Zhou, "An integrated giant magnetoimpedance biosensor for detection of biomarker," *Biosens. Bioelectron.*, vol. 58, pp. 338–344, 2014.

[12] H. Wang, Y. Chen, A. Hassibi, A. Scherer, and A. Hajimiri, "A frequency-shift CMOS magnetic biosensor array with single-bead sensitivity and no external magnet," in *IEEE Int. Solid-State Circuits Conf. Dig. Tech. Papers*, 2009, pp. 438–439, 439a.

[13] V. Luong, J. Jeng, B. Lai, J. Hsu, C. Chang, and C. Lu, "Design of three-dimensional magnetic field sensor with single bridge of spin-valve giant magnetoresistance films," in *Proc. IEEE Magn. Conf.*, 2015, pp. 1–1.

[14] T. Nakatani, S. Li, Y. Sakuraba, T. Furubayashi, and K. Hono, "Advanced CPP-GMR spin-valve sensors for narrow reader applications," *IEEE Trans. Magn.*, vol. 54, no. 2, Feb. 2018, Art. no. 3300211.

[15] S. Samyak and H. Heidari, "On-chip magnetoresistive sensors for detection and localization of paramagnetic particles," in *Proc. IEEE SENSORS Conf.*, Glasgow, U.K., 2017, pp. 1–3.

[16] P. R. Coulet, "What is a biosensor," in *Biosensor Principles and Applications*. Boca Raton, FL, USA: CRC, 1991, ch. 1, pp. 1–6.

[17] L. Marri, A. M. Jansson, C. E. Christensen, and O. Hindsgaul, "An enzyme-linked immunosorbent assay for the detection of diacetyl(2, 3-butanedione)," *Anal. Biochem.*, vol. 535, pp. 12–18, 2017.

[18] N. M. M. Pires, T. Dong, U. Hanke, and N. Hoivik, "Recent developments in optical detection technologies in lab-on-a-chip devices for biosensing applications," *Sensors*, vol. 14, pp. 15458–15479, 2014.

[19] L. Moro, M. Turemis, B. Marini, R. Ippodrino, and M. T. Giardi, "Better together: Strategies based on magnetic particles and quantum dots for improved biosensing," *Biotechnol. Adv.*, vol. 35, pp. 51–63, 2017.

[20] C. Albon, A. Weddemann, A. Auge, K. Rott, and A. Hütten, "Tunneling magnetoresistance sensors for high resolutive particle detection," *Appl. Phys. Lett.*, vol. 95, 2009, Art. no. 023101.

[21] J. Schotter, P. B. Kamp, A. Becker, A. Puhler, G. Reiss, and H. Bruckl, "Comparison of a prototype magnetoresistive biosensor to standard fluorescent DNA detection," *Biosens. Bioelectron.*, vol. 19, pp. 1149–1156, May 15, 2004.

[22] V. D. Krishna, K. Wu, A. M. Perez, and J.-P. Wang, "Giant magnetoresistance-based biosensor for detection of Influenza A Virus," *Front. Microbiol.*, vol. 7, pp. 1–8, 2016.

[23] S. M. Thompson, "The discovery, development and future of GMR: The nobel prize 2007," *J. Phys. D, Appl. Phys.*, vol. 41, 2008, Art. no. 093001.

[24] C.-C. Huang, X. Zhou, and D. A. Hall, "Giant magnetoresistive biosensors for time-domain magnetorelaxometry: A theoretical investigation and progress toward an immunoassay," *Sci. Rep.*, vol. 7, 2017, Art. no. 45493.

[25] R. S. Gaster, "Quantification of protein interactions and solution transport using high-density GMR sensor arrays," *Nature Nanotechnol.*, vol. 6, pp. 314–320, 2011.

[26] NVE Corp., "GMR sensors data book," Eden Prairie, MN, USA, 2003. [Online]. Available: https://www.nve.com/. [Accessed Feb. 25, 2018].

[27] Z. Zhu and D. Howe, "Halbach permanent magnet machines and applications: A review," in *Proc. IEEE Proc. Electr. Power Appl.*, 2001, vol. 148, pp. 299–308.

[28] O. Talcoth and T. Rylander, "Optimization of sensor positions in magnetic tracking," Chalmers Univ. Technol., Gothenburg, Sweden, 2011.

[29] A. Farajidavar, J. M. Block, and M. Ghovanloo, "A comprehensive method for magnetic sensor calibration: A precise system for 3-D tracking of the tongue movements," in *Proc. IEEE Eng. Med. Biol. Soc.*, 2012, pp. 1153–1156.

[30] B. Fry and R. Casey, *Processing*. [Online]. Available: https://processing.org/ [Accessed 2018].

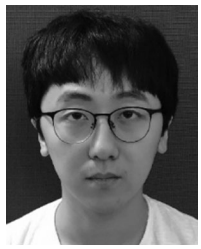

Zhaochen Yin (S'17) was born in Weifang, China, in 1994. He received the Bachelor's degree in electronic engineering in 2016 from the University of Liverpool, Liverpool, U.K., and the Master's degree in electronic engineering in 2017 from the University of Glasgow, Glasgow, U.K. In November 2018, he started working toward the Ph.D. degree with the University of Pavia in collaboration with STMicroelectronics (Studio di Microelettronica). His current research topic is high-speed ADC design.

Edoardo Bonizzoni (M'06) was born in Pavia, Italy, in 1977. He received the Laurea (*summa cum laude*) degree in electronic engineering and the Ph.D. degree in electronic, computer, and electrical engineering, with focus on the development, design, and testing of nonvolatile memories with particular regard to phase-change memories from the University of Pavia in 2002 and 2006, respectively. He has authored or coauthored more than 110 papers in international journals or conferences (with published proceedings) and two book chapters. Since 2006, his research interests have been mainly focused on the design and testing of dc–dc and A/D converters. He worked on single-inductor multiple-output dc–dc buck regulator solutions and on both Nyquist-rate and oversampled A/D converters. Recently, his research focuses on the design of high precision amplifiers, ultra-low-voltage voltage reference circuits, and sensor interfaces as well. He is currently a Senior Assistant Professor with the Department of Electrical, Computer, and Biomedical Engineering, University of Pavia. He was a co-recipient of the IEEE ISCAS 2014 Honorary Mention Paper Award of the Sensory Systems Track, the IEEE/IEEJ Analog VLSI Workshop 2010 Best Paper Award, the IEEE European Solid-State Circuits Conference 2007 Best Paper Award, and the IEEE/IEEJ Analog VLSI Workshop 2007 Best Paper Award. From 2011 to 2015, he served the IEEE Circuits and Systems Society as an Associate Editor for the IEEE TRANSACTIONS ON CIRCUITS AND SYSTEMS—PART II. Since 2016, he has been an Associate Editor for the IEEE TRANSACTIONS ON CIRCUITS AND SYSTEMS—PART I.

Hadi Heidari (SM'17) received the Ph.D. degree. He is a Lecturer with the School of Engineering, University of Glasgow. He leads the Microelectronics Lab (meLAB, www.gla.ac.uk/melab), and his research interests include microelectronics design, spintronics, and point-of-care diagnostics. He has authored more than 60 publications and has been recipient of awards from the IEEE NGCAS'17, ISSCC'16, PRIME'14, and ISCAS'14. He is an Editor for the *Microelectronics Journal* and a Guest Editor for four journal special issues. He is Board of Governors member of the IEEE Circuits and Systems Society and the IEEE Sensors Council AdCom.